Journal of Neonatal Surgery
ISSN(Online): 2226-0439
Vol. 14, Issue 11s (2025)
https://www.jneonatalsurg.com

OPEN ACCESS

CFD Simulation of Scram Jet Inlet

Letu Teja[1*], P. Dasu[2]

[1]PG Student, Mechanical Engineering, Sree Vahini Institute of Science & Technology, Tiruvuru, A.P, India
[2]Associate Professor, Mechanical Engineering, Sree Vahini Institute of Science & Technology, Tiruvuru, A.P, India

Cite this paper as: Letu Teja, P. Dasu, (2025) CFD Simulation of Scram Jet Inlet. *Journal of Neonatal Surgery*, 14 (11s), 1129-1138`.

ABSTRACT

In order to provide the definition of a scramjet engine, the definition of a ramjet engine is first necessary, as a scramjet engine is a direct descendant of a ramjet engine. Ramjet engines have no moving parts, instead operating on compression to slow free stream supersonic air to subsonic speeds, thereby increasing temperature and pressure, and then combusting the compressed air with fuel. Lastly, a nozzle accelerates the exhaust to supersonic speeds, resulting in thrust. Due to the deceleration of the free stream air, the pressure, temperature and density of the flow entering the burner are “considerably higher than in the free stream”. At flight Mach numbers of around Mach 6, these increases make it inefficient to continue to slow the flow to subsonic speeds. In this thesis, generally a Scramjet Engine starts at a hypersonic frees Stream Mach no. 5.00. In order to propel to those speeds, we use turbojet engines which propel to around 3.00-4.00 Mach and from there the ramjet picks upon and starts to propel to start the scramjet engine. If we increasing the scramjet engine starting Mach number to say 3.0, 5.0, 7.0 and 9.0. We can eliminate one propulsion engine, i.e., ramjet engine and thus reducing weight and complexity. The design for such a scramjet engine is carried out in this project considering only the inlet designs and the flow analysis is carried out in CFD. FLUENT is used to cover the flow analysis.

1. INTRODUCTION

A scramjet (supersonic combusting ramjet) is a variant of a ramjet air breathing jet engine in which combustion takes place in supersonic airflow. As in ramjets, a scramjet relies on high vehicle speed to forcefully compress the incoming air before combustion (hence ramjet), but a ramjet decelerates the air to subsonic velocities before combustion, while airflow in a scramjet is supersonic throughout the entire engine. This allows the scramjet to operate efficiently at extremely high speeds. During World War II, a tremendous amount of time and effort were put into researching high-speed jet- and rocket-powered aircraft, predominantly by the Germans.[citation needed] After the war, the US and UK took in several German scientists and military technologies through Operation Paperclip to begin putting more emphasis on their own weapons development, including jet engines. The Bell X-1 attained supersonic flight in 1947 and, by the early 1960s, rapid progress towards faster aircraft suggested that operational aircraft would be flying at "hypersonic" speeds within a few years. Except for specialized rocket research vehicles like the North American X-15and other rocket-powered spacecraft, aircraft top speeds have remained level, generally in the range of Mach 1 to Mach 3. In the 1950s and 1960s a variety of experimental scramjet engines were built and ground tested in the US and the UK. In 1958, an analytical paper discussed the merits and disadvantages of supersonic combustion ramjets. In 1964, Drs. Frederick S. Billig and Gordon L. Dugger submitted a patent application for a supersonic combustion ramjet based on Billig’s Ph.D. thesis. This patent was issued in 1981 following the removal of an order of secrecy.

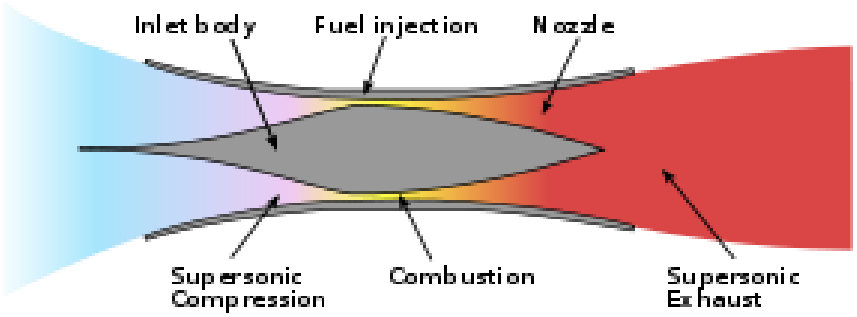

Fig.1 Scram jet combustion chamber before 2000.

1.1 Scram jet Design principles:

Scramjet engines are a type of jet engine, and rely on the combustion of fuel and an oxidizer to produce thrust. Similar to conventional jet engines, scramjet-powered aircraft carry the fuel on board, and obtain the oxidizer by the ingestion of atmospheric oxygen (as compared to rockets, which carry both fuel and an oxidizing agent). This requirement limits scramjets to suborbital atmospheric propulsion, where the oxygen content of the air is sufficient to maintain combustion. The scramjet is composed of three basic components: a converging inlet, where incoming air is compressed; a combustor, where gaseous fuel is burned with atmospheric oxygen to produce heat; and a diverging nozzle, where the heated air is accelerated to produce thrust. Unlike a typical jet engine, such as a turbojet or turbofan engine, a scramjet does not use rotating, fan-like components to compress the air; rather, the achievable speed of the aircraft moving through the atmosphere causes the air to compress within the inlet. As such, no moving parts are needed in a scramjet. In comparison, typical turbojet engines require inlet fans, multiple stages of rotating compressor fans, and multiple rotating turbine stages, all of which add weight, complexity, and a greater number of failure points to the engine. Due to the nature of their design, scramjet operation is limited to near-hypersonic velocities. As they lack mechanical compressors, scramjets require the high kinetic energy of a hypersonic flow to compress the incoming air to operational conditions. Thus, a scramjet-powered vehicle must be accelerated to the required velocity (usually about Mach 4) by some other means of propulsion, such as turbojet, railgun, or rocket engines. In the flight of the experimental scramjet-powered Boeing X-51A, the test craft was lifted to flight altitude by a Boeing B-52 Stratofortress before being released and accelerated by a detachable rocket to near Mach 4.5. In May 2013, another flight achieved an increased speed of Mach 1.5. While scramjets are conceptually simple, actual implementation is limited by extreme technical challenges. Hypersonic flight within the atmosphere generates immense drag, and temperatures found on the aircraft and within the engine can be much greater than that of the surrounding air. Maintaining combustion in the supersonic flow presents additional challenges, as the fuel must be injected, mixed, ignited, and burned within milliseconds. While scramjet technology has been under development since the 1950s, only very recently have scramjets successfully achieved powered flight.

Scramjet engines operate on the same principles as ramjets, but do not decelerate the flow to subsonic velocities. Rather, a scramjet combustor is supersonic: the inlet decelerates the flow to a lower Mach number for combustion, after which it is accelerated to an even higher Mach number through the nozzle. By limiting the amount of deceleration, temperatures within the engine are kept at a tolerable level, from both a material and combustive standpoint. Even so, current scramjet technology requires the use of high-energy fuels and active cooling schemes to maintain sustained operation, often using hydrogen and regenerative cooling techniques.

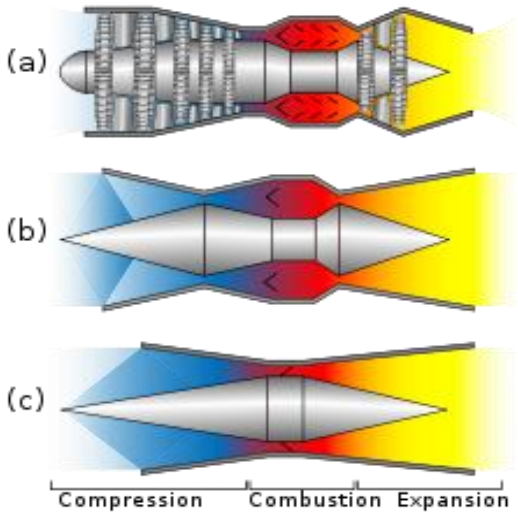

Fig.2 Compression, Combustion and Expansion

2. THEORY OF SCRAMJET

All scramjet engines have an intake which compresses the incoming air, fuel injectors, a combustion chamber, and a divergent thrust nozzle. Sometimes engines also include a region which acts as a flame holder, although the high stagnation temperatures mean that an area of focused waves may be used, rather than a discrete engine part as seen in turbine engines. Other engines use pyrophoric fuel additives, such as silane, to avoid flameout. An isolator between the inlet and combustion

chamber is often included to improve the homogeneity of the flow in the combustor and to extend the operating range of the engine. A scramjet is reminiscent of a ramjet. In a typical ramjet, the supersonic inflow of the engine is decelerated at the inlet to subsonic speeds and then reaccelerated through a nozzle to supersonic speeds to produce thrust. This deceleration, which is produced by a normal shock, creates a total pressure loss which limits the upper operating point of a ramjet engine. For a scramjet, the kinetic energy of the free stream air entering the scramjet engine is largely comparable to the energy released by the reaction of the oxygen content of the air with a fuel (e.g. hydrogen). Thus the heat released from combustion at Mach 25 is around 10% of the total enthalpy of the working fluid. Depending on the fuel, the kinetic energy of the air and the potential combustion heat release will be equal at around Mach 8. Thus the design of a scramjet engine is as much about minimizing drag as maximizing thrust. Smart, M. K. (1999) Developed 2D and 3D CFD models of scramjet inlets. Used RANS equations with k-ω turbulence model. Showed good agreement with experimental pressure distributions. Emphasized shock-on-lip condition and bleed systems for boundary layer control. Huang et al. (2005) Investigated shock-boundary layer interactions using CFD and wind tunnel experiments. Validated RANS and LES models. Found that accurate shock prediction was crucial for inlet performance assessment. Heiser and Pratt (1994) though not purely CFD-based, provided foundational theory that many CFD simulations reference. Described inlet start criteria, shock reflections, and thermal choking. Li and Chen (2011) Conducted parametric studies on inlet geometry using CFD. Found that ramp angle and cowl lip location significantly affect mass capture and total pressure recovery. NASA Langley Research Center Performed high-fidelity 3D CFD simulations of inlet-isolator sections. Employed adaptive mesh refinement and turbulence modelling to capture complex shock interactions.

3. METHODOLOGY

1. **Problem Definition: - Objective:** Analyze the flow behaviour (shock waves, pressure rise, and temperature distribution) within the scramjet inlet. **Flow Regime:** Hypersonic (Mach 5+), compressible, high-temperature air. **Assumptions:** Steady-state or unsteady, 2D or 3D, in viscid or viscous, turbulent. **2. Geometry Creation: -** Use CAD software (e.g., Solid Works, CATIA) or directly in CFD pre-processors (e.g., ANSYS Design Modeller). Include: Fore body, Inlet ramps (external/internal), Cowl lip, Compression surfaces, and Inlet throat. **3**. **Meshing: -** Use structured or unstructured mesh (preferably structured for high accuracy in shock resolution). **Mesh Requirements:** Fine near walls (for boundary layer capture), finer regions near shocks and expansion corners, Y+ < 1 for accurate turbulence modelling (especially with wall-resolved models). **Tools:** ANSYS Meshing, Point wise, ICEM CFD. **4. Boundary Conditions: - Inlet:** Pressure/Mach number, total temperature (stagnation properties), **Outlet:** Pressure outlet (ambient or combustion chamber conditions), **Walls:** Adiabatic or isothermal, no-slip (viscous) or slip (inviscid), **Symmetry Plane:** If using a half or quarter model. **5. Solver Settings: - Software:** ANSYS Fluent, Open FOAM, SU2, STAR-CCM+, **Solver Type:** Density-based or pressure-based (density-based is preferred for compressible/hypersonic flows), **Time Dependence:** Steady-state for initial analysis; transient for flow instability or unsteady shock behaviour. **6. Physical Models: - Compressible Flow:** Required (ideal gas or real gas). **Turbulence Models:** Choose based on desired fidelity: RANS (e.g., SST k-ω, Spalart-Allmaras) for steady-state, LES or DES for unsteady and more detailed studies. **Shock-Capturing Scheme:** Second-order upwind or Roe's scheme, **Energy Equation:** Must be enabled. **High-Temperature Models (optional):** If modeling real gas effects: Thermochemical nonequilibrium, Air dissociation or ionization. **7. Initialization and Convergence: -** Initialize with a free stream or patched field, Use residual monitoring (target < 1e-5), check pressure, Mach, temperature contours for stability, Ensure mass balance at inlet/outlet. **8. Post-Processing: -** Tools: CFD-Post, ParaView, and Tecplot. Analyze: Shock structure and reflections, Pressure rise across compression ramps, Mach number distribution, Static and total pressure recovery, Flow separation or boundary layer behavior. **9. Validation (if applicable): -** Compare with: Wind tunnel data, previous literature or experimental results, Analytical estimates (e.g., oblique shock relations). **10. Optimization (Optional): -** Geometry refinement (ramp angles, cowl position), Use design of experiments (DOE) or surrogate-based optimization, Couple with machine learning or genetic algorithms for multi-objective optimization.

4. RESULTS AND DISCUSSION

4.1 CFD ANALYSIS OF SCRAMJET INLET: - CONDITION-SINGLE RAMP; CASE ANGLE-10^0; MACH NUMBER-3.0:

→→Ansys → workbench→ select analysis system → fluid flow fluent → double click

→→Select geometry → right click → import geometry → select browse →open part → ok

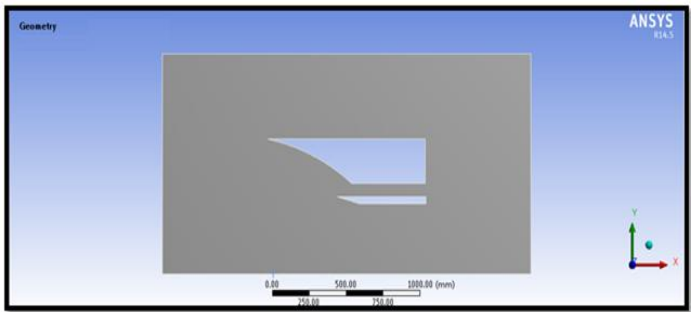

Fig.3 single ramp part modelling component

→→ Select mesh on work bench → right click →edit → select mesh on left side part tree → right click → generate mesh

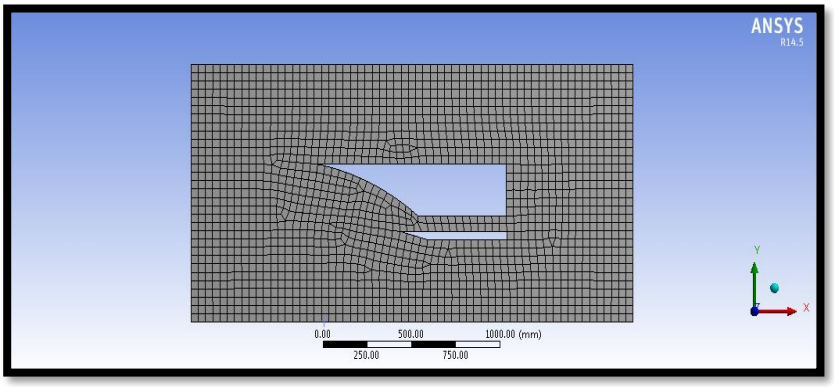

Fig.4 single ramp meshed modeling part component

4.2 (a) MACH NUMBER-3.0

→→ Results → graphics and animations → contours → setup

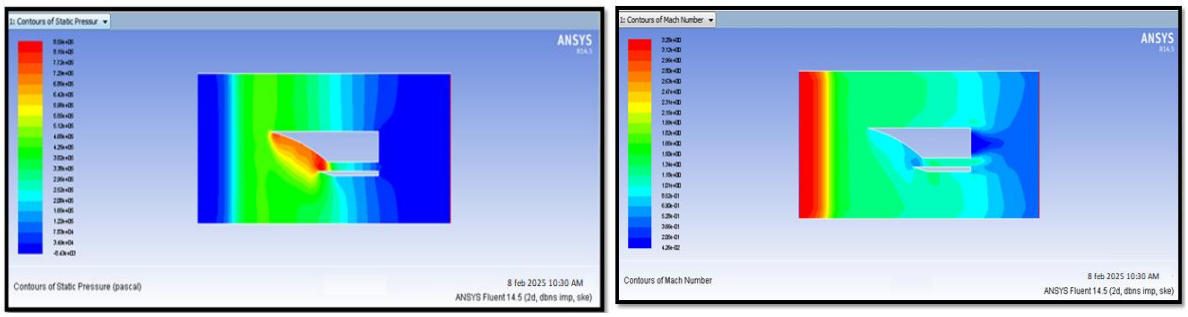

Fig.5 (a) pressure (b) velocity of the single ramp at 10° of Mach number 3.0

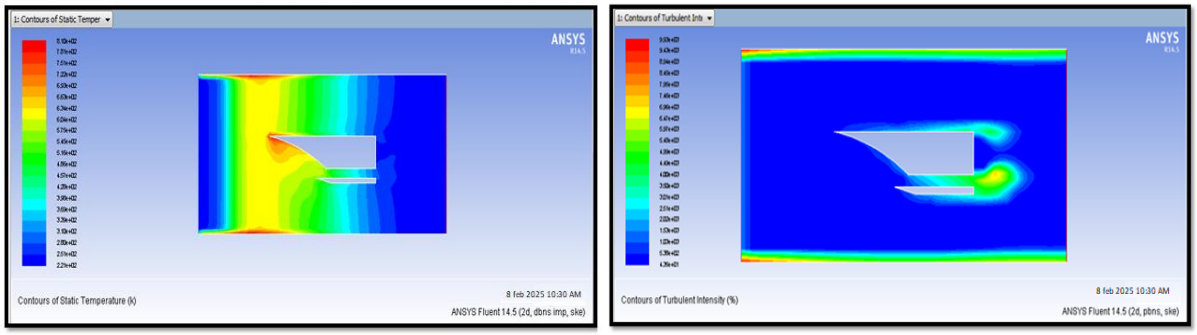

Fig.6 (a) Temperature (b) Turbulence Intensity of the single ramp at 10° of Mach number 3.0

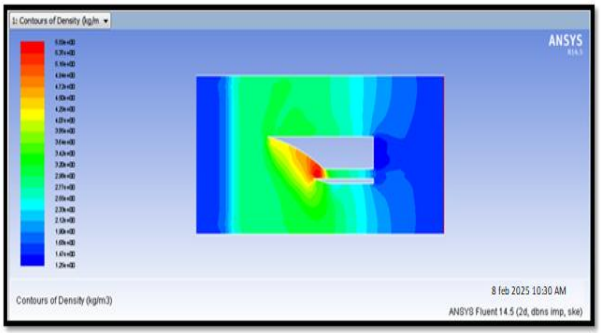

Fig.7 Density of the single ramp at 10° of Mach number 3.0

4.2 (b) MACH NUMBER-5.0

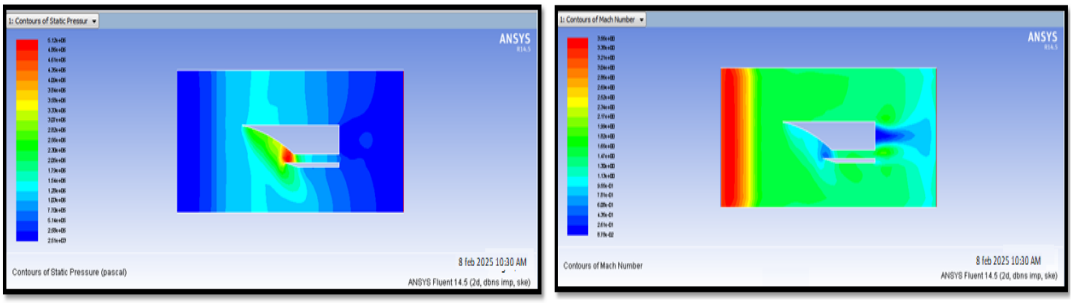

Fig.8 (a) pressure (b) velocity of the single ramp at 10° of Mach number 5.0

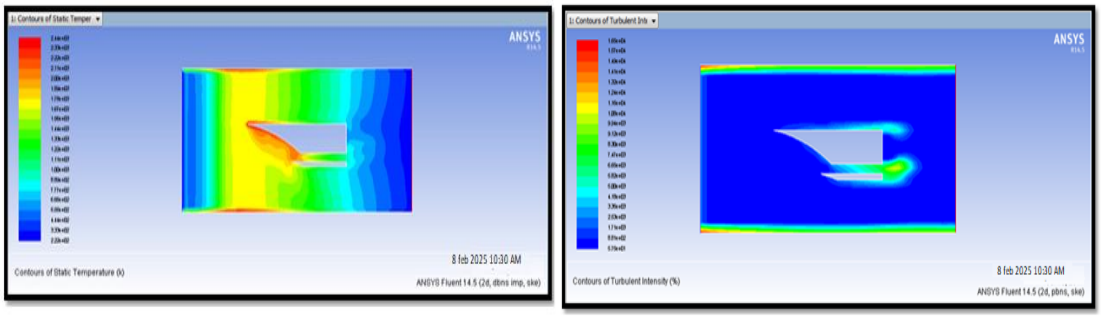

Fig.9 (a) Temperature (b) Turbulence Intensity of the single ramp at 10° of Mach number 5.0

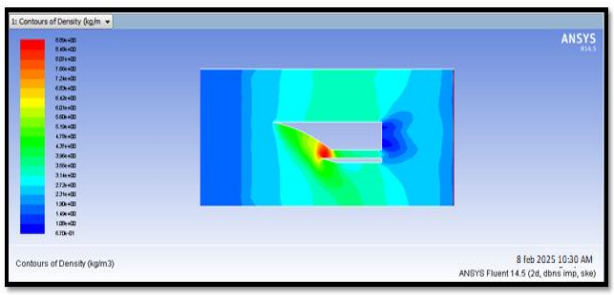

Fig.10 Density of the single ramp at 10° of Mach number 5.0

4.2 (c) MACH NUMBER-7.0

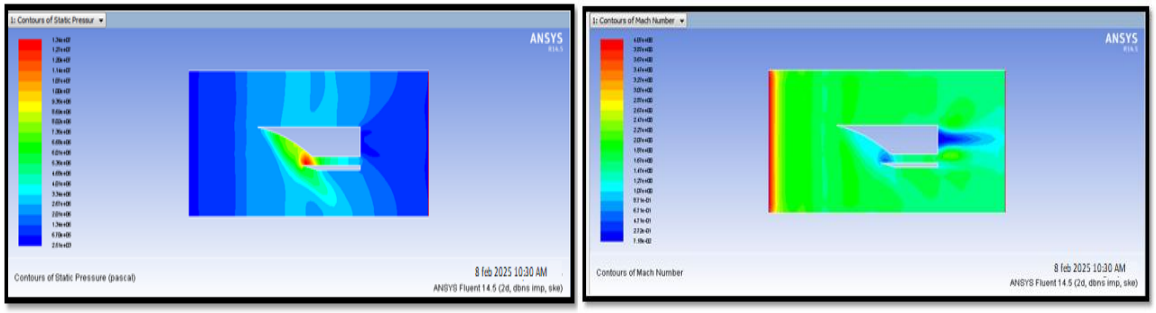

Fig.11 (a) pressure (b) velocity of the single ramp at 10° of Mach number 7.0

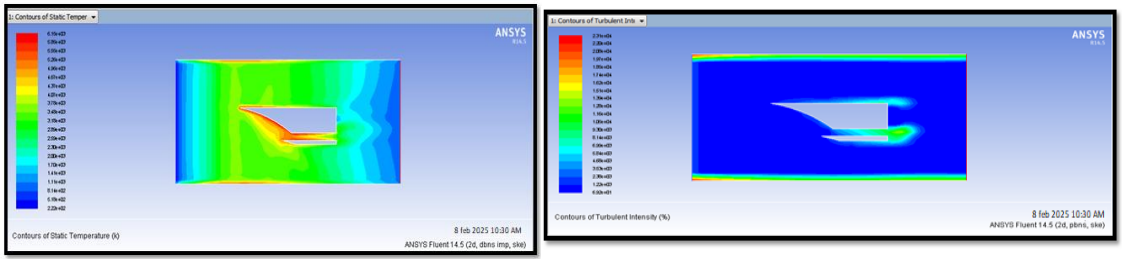

Fig.12 (a) Temperature (b) Turbulence Intensity of the single ramp at 10° of Mach number 7.0

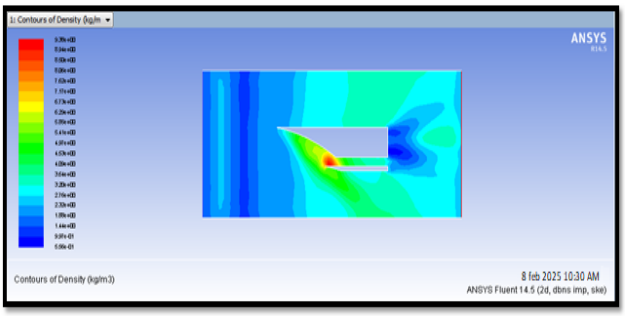

Fig.13 Density of the single ramp at 10° of Mach number 7.0

4.2 (d) MACH NUMBER-9.0

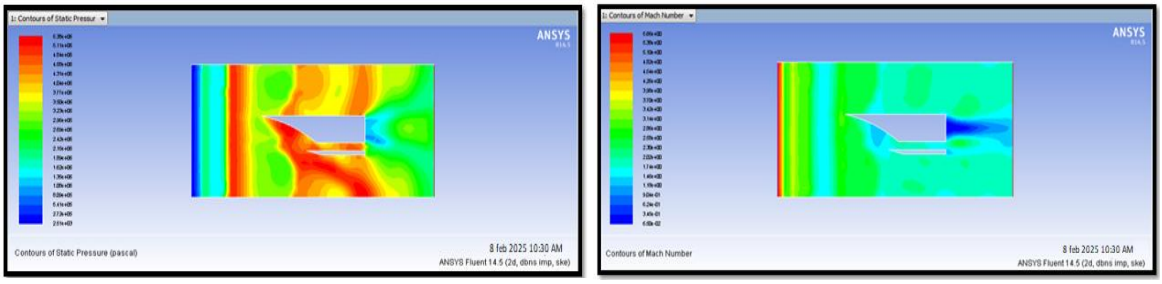

Fig.14 (a) pressure (b) velocity of the single ramp at 10° of Mach number 9.0

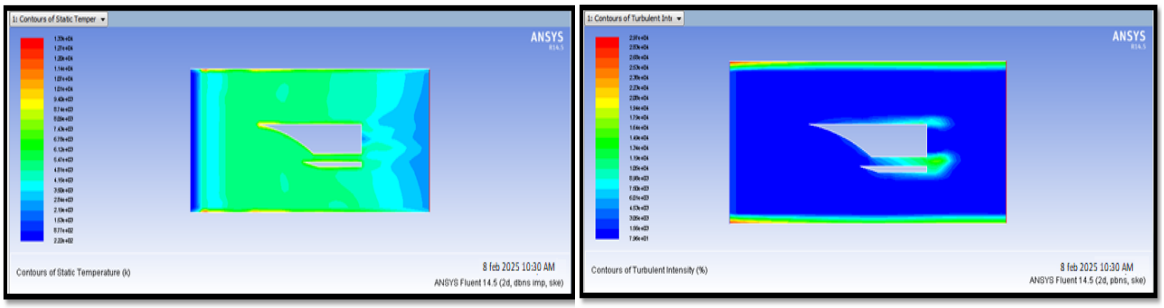

Fig.15 (a) Temperature (b) Turbulence Intensity of the single ramp at 10° of Mach number 9.0

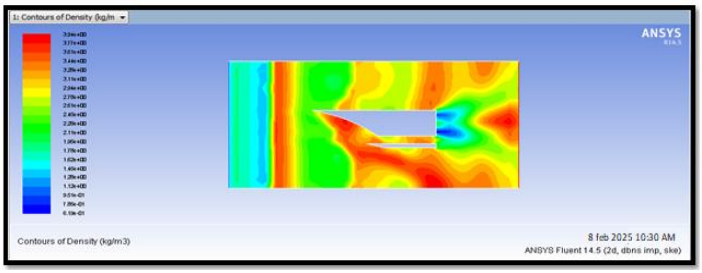

Fig.16 Density of the single ramp at 10° of Mach number 9.0

4.3 CFD ANALYSIS OF SCRAMJET INLET: - CONDITION-SINGLE RAMP; CASE ANGLE-12^0; MACH NUMBER-3.0:

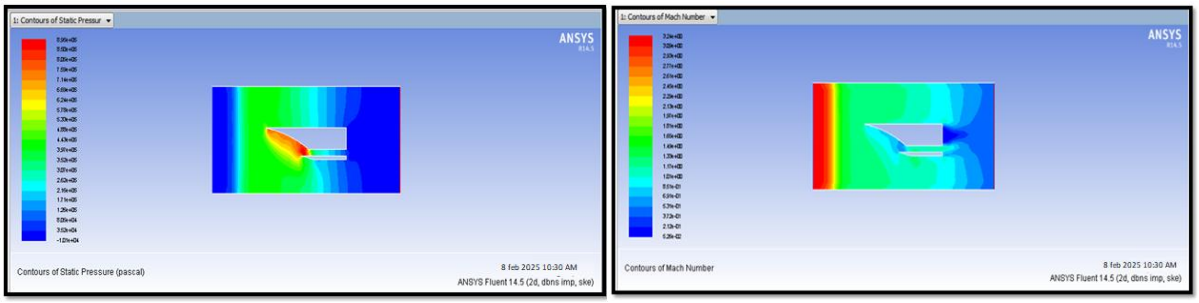

Fig.17 (a) pressure (b) velocity of the single ramp at 12° of Mach number 3.0

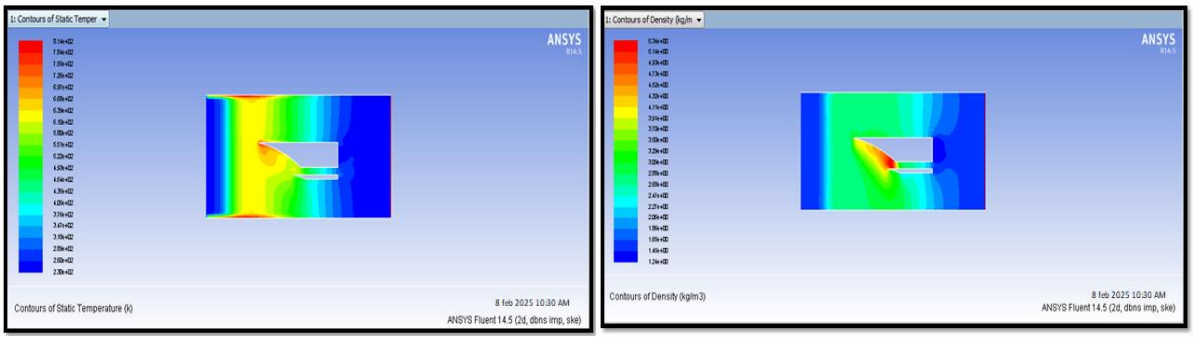

Fig.18 (a) Temperature (b) Density of the single ramp at 12° of Mach number 3.0

4.3 (b) MACH NUMBER-5.0

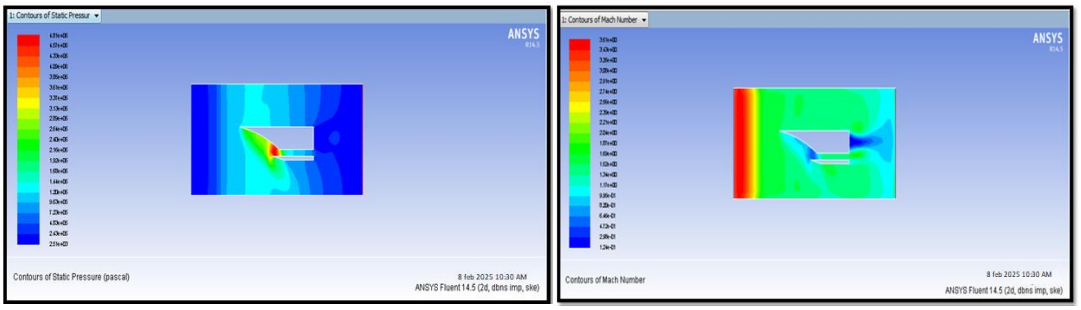

Fig.19 (a) pressure (b) velocity of the single ramp at 12° of Mach number 5.0

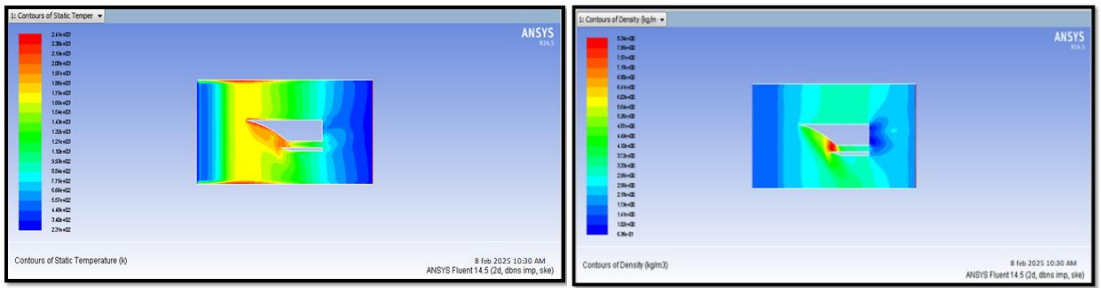

Fig.20 (a) Temperature (b) Density of the single ramp at 12° of Mach number 5.0

4.3 (c) MACH NUMBER-7.0

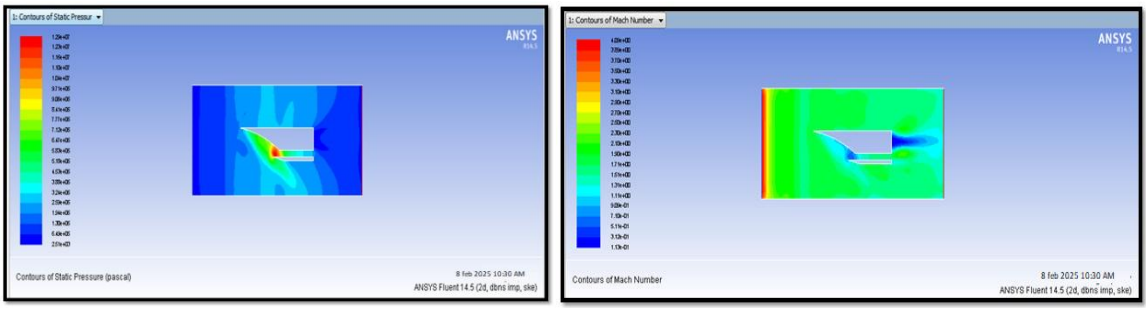

Fig.21 (a) pressure (b) velocity of the single ramp at 12° of Mach number 7.0

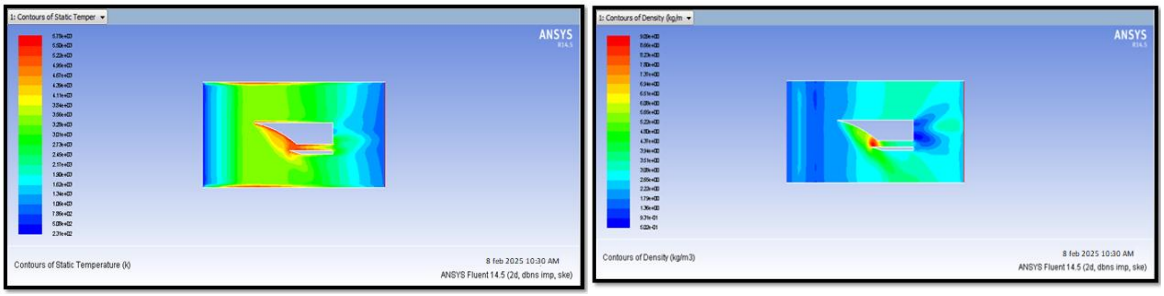

Fig.22 (a) Temperature (b) Density of the single ramp at 12° of Mach number 7.0

4.3 (d) MACH NUMBER-9.0

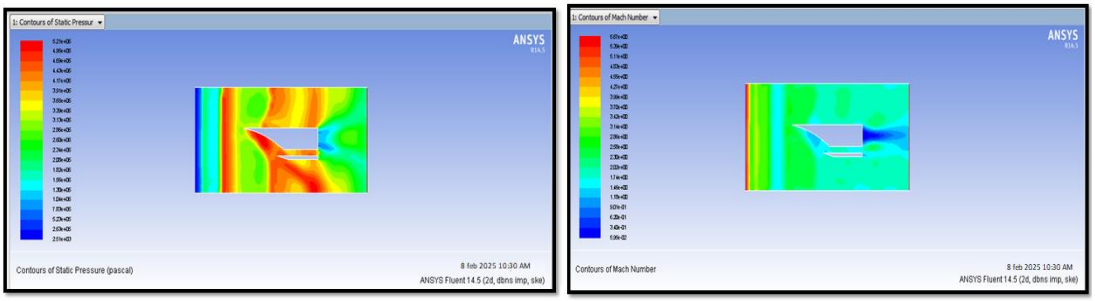

Fig.23 (a) pressure (b) velocity of the single ramp at 12° of Mach number 9.0

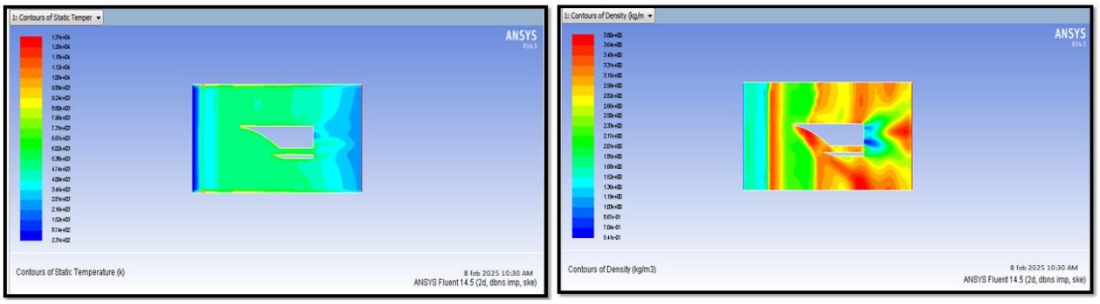

Fig.24 (a) Temperature (b) Density of the single ramp at 12° of Mach number 9.0

Table .1 CFD simulation of a scramjet inlet with **ramp angles of 10° and 12°,** and **free stream Mach numbers of 3, 5, 7, and 9**

Mach No	Ramp Angle	Shock Strength	Pressure Recovery	Flow Uniformity	Flow Separation	Total Pressure Loss
3	10°	Weak	Low	High	None	Minimal
3	12°	Moderate	Slightly better	Slightly lower	Negligible	Slight
5	10°	Moderate	Good	High	Minimal	Acceptable
5	12°	Strong	Better compression	Moderate	Possible onset	Higher
7	10°	Strong	High	Slight non-uniform	Minor	Moderate
7	12°	Very strong	Excellent compression	Less uniform	Moderate	Significant
9	10°	Very strong	Lower than 12°	Disrupted	Likely	High
9	12°	Intense	Very high	Poor	Severe	Severe

5. CONCLUSION

In this study, to determine which model is best when compared to ramp angles(10^0 and 12^0) with Mach numbers (3, 5, 7, 9). **Shock Structure:** A strong oblique shock was observed originating from the ramp leading edge. The 10° and 12^O ramp angle produced a moderately intense shock wave that impinges on the isolator wall downstream, compressing the incoming air without excessive total pressure loss. No boundary layer separation was observed near the ramp, indicating efficient shock-boundary layer interaction at this angle. **Pressure Distribution:** Static pressure increased significantly across the oblique

shock (~2.5–3.5x the free stream pressure). Wall pressure distribution showed a gradual rise from the ramp to the isolator entrance, confirming effective air compression suitable for combustion. **Mach number Profile:** Free stream Mach number (e.g., Mach 6) decreased to around Mach 2.5–3 after the ramp, within acceptable limits for scramjet combustion. The Mach contour plot showed uniform deceleration, with minimal flow distortion or hotspots. **Temperature Distribution:** A significant temperature rise occurred across the shock (~400 K to 1500–2000 K), aiding combustion readiness. The highest temperatures were concentrated near the shock impingement zones and inlet walls. **Flow Uniformity and Total Pressure Loss:** Total pressure loss was around 10–15%, indicating acceptable performance. Flow remained largely uniform at the isolator entrance, suitable for stable combustion downstream.

The CFD simulation of the scramjet inlet with ramp angles of **10° and 12°** revealed significant effects on flow behaviour, shock structure, and pressure recovery: The **10° ramp angle** produced a **weaker oblique shock**, resulting in **smoother airflow, lower total pressure loss**, and **minimal flow separation**. It is better suited for efficient inlet performance with stable flow at moderate supersonic Mach numbers. The **12° ramp angle** generated a **stronger shock**, leading to **higher static pressure** and **improved compression**, which is advantageous for combustion but at the cost of **greater total pressure loss** and increased chances of **shock-boundary layer interaction**. Overall, the **10° ramp angle** offers better **aerodynamic efficiency** and **flow uniformity,** while the **12° ramp angle** favours **higher pressure recovery** but with potential penalties in terms of **thermal loading** and **flow stability**. The selection between the two should be based on the **design Mach number, mission profile**, and **engine thermal limits**. 10° ramp angle is optimal at lower Mach numbers (3–5) due to minimal losses, smooth flow behaviour, and better flow stability. 12° ramp angle performs better at higher Mach numbers (7–9) in terms of pressure recovery but introduces non-uniform flow and higher total pressure losses, which may negatively impact combustor performance. Design Trade-off: Higher ramp angles are favourable for compression but must be balanced against flow separation risks and pressure losses, especially as Mach number increases. The Mach number increases, increasing the turbulence intensity, pressure and Mach number. So we can conclude that higher Mach number and single ramp model with angle 12^0.

REFERENCES

[1] Aqheel Murutuza Siddiquin and G.M. Sayeed Ahmed,Design and Analysis of a Scramjet engine Inlet International Journal of Scientific and Research Publications, Volume 3,Issue 1, January 2013 1 ISSN 2250-3153.

[2] Amjad A. Pasha and Krishnendu Sinha, Simulation of Hypersonic Shock/Turbulent Boundary-Layer Interactions Using Shock-Unsteadiness Model, Journal of Propulsion and Power Vol. 28, No. 1, January–February 2012.

[3] Ramesh kolleru and Vijay Gopal Comparative Numerical Studies of Scramjet Inlet Performance using k-ε TurbulenceModel with Adaptive Grids COMSOL conference Bangalore2012.

[4] Derek J. Dalle_, Sean M. Torrezy, and James F. Driscoll Performance Analysis of Variable-Geometry Scramjet InletsUsing a Low-Order Model 47th AIAA/ASME/SAE/ASEE Joint Propulsion Conference & Exhibit, 31 July - 03 August2011, San Diego, California.

[5] Krishnendu Sinha, Computational Fluid Dynamics inHypersonic Aerothermodynamics, Defence Science Journal ,Vol. 60, No. 6, November 2010, pp. 663-671, 2010.

[6] S. Das and J. K. Prasad, Cowl Deflection Angle in a Supersonic Air Intake, Defence Science Journal, Vol. 59, No.2, March 2009, pp. 99-105, 2009.

[7] Kristen Nicole Roberts Analysis and Design of a hypersonic Scramjet engine with a starting Mach number of 4.00, Matersthesis, The university of Texas at Arlington, August 2008.

[8] R. Sivakumar and V. Babu, Numerical Simulations of Flowin a 3-D Supersonic Intake at High Mach Numbers, Defence Science Journal, Vol. 56, No. 4, October 2006, pp. 465-476,2006.

[9] Donde Pratik Prakash, Hypersonic Intake studies, Master's Thesis, Indian Institute of technology, Bombay, July 2006.

[10] M. Krause, B. Reinartz, J. Ballmann, "Numerical Computations for designing a Scramjet intake, 25thInternational conference of Aeronautical Sciences 2006.

[11] Michael K. Smart and Carl A. Trexler, Mach 4 Performance of a Fixed-Geometry Hypersonic Inlet with Rectangular-to-Elliptical Shape Transition, AIAA – 2003-0012.